ACS EARTH AND SPACE CHEMISTRY

Article

Cite This: ACS Earth Space Chem. 2019, 3, 2472−2481

http://pubs.acs.org/journal/aesccq

Heterocyclic Product Formation in Aqueous Brown Carbon Systems

Daisy N. Grace,[‡] Jacqueline R. Sharp,[‡] Rachael E. Holappa, Emily N. Lugos, Melissa B. Sebold,[†] Daniel R. Griffith, Heidi P. Hendrickson, and Melissa M. Galloway*

Department of Chemistry, Lafayette College, Easton, Pennsylvania 18042, United States

Supporting Information

ABSTRACT: Brown carbon in aerosol remains a significant source of error in global climate modeling due to its complex nature and limited product characterization. Though significant efforts have been made in the previous decade to identify the major light-absorbing brown carbon chromophores formed through the reactions of carbonyl-containing compounds with ammonium, substantial work is still required to identify the main absorbing species resulting from reactions of glyoxal, glycolaldehyde, and hydroxyacetone with ammonium sulfate (AS). Using tandem mass spectrometry and ^{15}N experiments to confirm proposed structures and support their mechanistic pathways, compelling evidence is provided for the formation of pyrazines and imidazoles in the glyoxal + AS, glycolaldehyde + AS, and hydroxyacetone + AS systems. Through density functional theory calculations, the N-containing oligomers and aromatic heterocycles formed within these reaction systems are shown to contribute to brown carbon light absorption, thus holding significant relevance toward accurately predicting their effects on global climate.

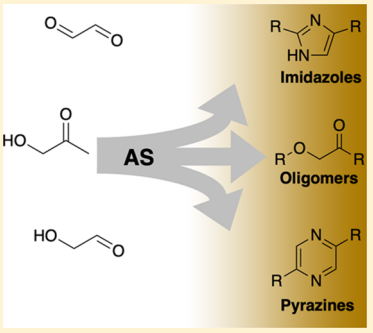

KEYWORDS: *brown carbon aerosol, glyoxal, glycolaldehyde, hydroxyacetone, ammonium sulfate, pyrazines, imidazoles*

1. INTRODUCTION

Aqueous aerosol particles can take up small, water-soluble carbonyl compounds,[1−4] which undergo Maillard-type browning reactions with ammonium salts and amines to produce nitrogen-containing heterocycles and oligomers capable of absorbing solar radiation.[5−7] The carbonyl-containing compounds methylglyoxal (MGly), glyoxal (Gly), glycolaldehyde (GAld), and hydroxyacetone (HA) have been identified as atmospheric organic compounds capable of these reactions (see Figure 1). These carbonyl species are abundant in the atmosphere, originating primarily from the gas-phase oxidation of biogenic and anthropogenic volatile organic compounds.[8−11] Ammonium ions, primary amines, and amino acids have all been shown to nucleophilically attack at the carbonyl carbon, effectively promoting the aldol condensation and intramolecular cyclization pathways that produce the imines, N-heterocycles, and aromatic compounds that act as the major contributors to brown carbon (BrC) light absorption in the atmosphere.[6,7,12−25]

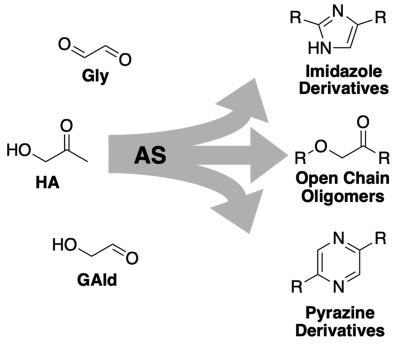

Figure 1. Small water-soluble carbonyl compounds react with ammonium sulfate to produce atmospheric BrC.

MGly and Gly, the two simplest and most abundant α-dicarbonyls in the atmosphere, have been extensively studied, and mechanistic pathways and structural characteristics of several classes of their resultant BrC chromophores have been identified.[6,9,14,16,18,19,21,26−29] The carbonyl groups on MGly and Gly enable intramolecular reactions to form heterocyclic products like pyridines, pyrazines, and, most notably, imidazole derivatives.[7,9,11,13,17,29,30] Along with open-chain reduced N-containing oligomers, these species comprise the majority of the chromophoric behavior in these carbonyl + AS systems.[19] For the Gly + AS system, Nozière et al. found that oligomerization occurs via ammonium-catalyzed formation of acetals followed by imine formation and subsequent oligomerization to open chains or heterocycles.[15] Thus, the primary BrC products from the Gly + AS system are imidazoles and diamines.[22] Kampf et al. further characterized the contributions of BrC chromophores in the Gly + AS system by identifying trace levels of biimidazole as the major contributor to the absorption band at 280 nm,[18] thus emphasizing the importance of identifying even small concentrations of BrC chromophore structures within organic aerosol mass if they have large absorption coefficients.[9,16] The

Received: September 2, 2019
Revised: September 18, 2019
Accepted: September 19, 2019
Published: September 19, 2019

DOI: 10.1021/acsearthspacechem.9b00235
ACS Earth Space Chem. 2019, 3, 2472−2481

MGly + AS system forms similar products, yet these products are more structurally inclined to follow mechanistic oligomerization routes through aldol condensation pathways rather than acetal formation,[11,17] and forms analogous methylimidazole products to the Gly + AS reaction system.[17] In addition to imidazole derivatives, Hawkins et al. also identified novel pyrazine derivatives in the MGly + AS system.[30] High water content may suppress the formation of these compounds, which may explain why they were not previously observed in studies of bulk, aqueous atmospheric mimics that did not involve an evaporation step.[30] These chromophoric species may contribute to previously unexplained light absorption in this carbonyl + AS system.[19]

Powelson et al. conducted experiments that show the relative amounts of BrC production in carbonyl + AS systems as follows: MGly > Gly > GAld > HA.[7] Though they contribute to less BrC production than MGly in controlled reactions containing identical carbonyl + AS concentrations, Gly, GAld, and HA are still relevant in studies regarding BrC due to their abundance in the atmosphere. Gly is 1.5 times more abundant on average than MGly in cloud and aqueous aerosol droplets and is commonly used as a tracer for secondary organic aerosol formation in atmospheric models.[7,14,31] GAld and MGly are found in nearly equal concentrations in the atmospheric condensed phase.[7] Though HA is far less abundant than GAld in the atmosphere, the HA + AS system can contribute to twice the absorbance as the GAld + AS system in the 200 to 300 nm range, thus elevating its relative potential for BrC production.[7] Therefore, it is essential to identify the major BrC chromophores in these lesser-understood carbonyl + AS systems in order to accurately account for BrC production in global climate models.

Aldol condensation is not likely to be a significant oligomerization pathway for GAld in the presence of ammonium due to poor catalytic activity of AS in this system.[7] While Powelson et al. surmised that GAld + AS systems in the presence of formaldehyde could form pyrazine and pyridine derivatives, these assertions have yet to be confirmed with experimental analysis.[7] Yi et al. also analyzed the GAld + AS reaction system, concluding that GAld follows similar BrC product formation as the α-dicarbonyl + AS systems, where nucleophilic attack by AS (or an amine) precedes aldol self-condensation and dehydration in order to form oligomers and higher molecular weight products.[25] They reported the major absorption products as open-chain imine- and carbonyl-containing oligomers. Most notably, Yi et al. proposed that the lack of a second carbonyl group in GAld prevents it from forming cyclic aromatic compounds like imidazole in its reaction with glycine.[25]

De Haan et al. reported that HA + AS will only produce sufficient products to contribute to aerosol yields if HA participates in oligomerization reactions, mainly with MGly.[12] However, its structural similarities to MGly and GAld may allow the HA + AS system to undergo similar acetal and amination reactions to α-dicarbonyl + AS and GAld + AS, resulting in the formation of BrC compounds. To the authors' knowledge, no reaction products have been proposed for the HA + AS reaction system.[32]

Much is still unknown about the reactions of AS with Gly, GAld, and HA. These reaction systems are likely to undergo similar initial reactions with ammonia in solution and to form aldol and acetal oligomers as well as imidazole and pyrazine products. To characterize the highly polar, complex compounds originating from each of these carbonyl + AS systems, supercritical fluid chromatography−tandem mass spectrometry (SFC-MS/MS) and ^{15}N-AS isotopic substitution experiments were utilized to separate and analyze these reaction mixtures for structural identification.

2. MATERIALS AND METHODS

2.1. Reagents. Glyoxal (40% w/w in H_2O) and hydroxyacetone (95%) were obtained from Alfa Aesar, and glycolaldehyde dimer and ammonium sulfate were purchased from Sigma-Aldrich. For the isotopic substitution (^{15}N) experiments, ^{15}N-AS (99%) was purchased from Cambridge Isotope Laboratories, Inc. Food grade carbon dioxide was obtained from Airgas. Methanol (Optima LC/MS grade) and formic acid (Optima LC/MS grade) were purchased from Fisher Chemical.

2.2. Preparation of Carbonyl and Ammonium Sulfate Mixtures. Separate standard solutions of 1 M each of GAld, Gly, HA, AS, and ^{15}N-AS were prepared in Millipore Milli-Q Ultrapure water (Milli-Q, 18.2 MΩ cm resistivity) and used within 1 month. Solutions containing 50 mM carbonyl + 50 mM AS were prepared from the stock solutions using Milli-Q water and evaporated until dry at 40 °C using a Buchi Rotavapor RII to simulate atmospheric cloud processing.[22] An analogous set of 50 mM carbonyl + 50 mM ^{15}N-AS solutions was prepared for the ^{15}N experiments. The solutions were reconstituted back to their original volume using Milli-Q water for analysis via SFC-MS/MS.

2.3. SFC-MS/MS. All samples were analyzed immediately after reconstitution using a Waters ACQUITY Ultra Performance Chromatography (UPC^2) supercritical fluid chromatography system coupled to a Waters XEVO TQD tandem quadrupole mass spectrometer. Further details about this instrument and chromatography technique can be found in the study of Grace et al.[33]

A binary gradient of CO_2 and methanol was used for elution of all samples through an ACQUITY UPLC BEH Amide column (2.1 × 50 mm, 1.7 μm particles). Starting conditions of 99% CO_2 and 1% methanol were held for 2 min, and then the modifier content was increased to 45% over 18 min and then held at 45% until 26 min before the system returned to initial conditions for 3 min. The total flow rate was held constant at 1.0 mL/min with 0.25 mL/min MeOH + 1.0% formic acid makeup flow. The UPC^2 system back pressure was set to 1500 psi throughout the duration of all sample runs. All data were collected in positive ESI mode. ESI conditions were set as follows: capillary voltage = 1.18 kV, cone voltage = 30 V, desolvation temperature = 200 °C, desolvation gas flow = 650 L/h, and cone flow = 1 L/h. Once a mass was identified in the mass spectrum, the sample was reanalyzed using extracted ion chromatography (EIC) to provide better sensitivity. Tandem mass spectrometry was also utilized to determine structural features.

2.4. Computational Methods. Density functional theory calculations were carried out for all compounds at the wB97X-D[34,35]/6-311G(2d, p)[36,37] level using Gaussian 16.[38] The ground-state geometry was optimized for each compound, and a frequency calculation was performed to confirm the energy was at a minimum on the potential energy surface. Time-dependent density functional theory (TDDFT) was used to calculate the 15 lowest-lying excitations per compound. All calculations utilized a conductor-like polarizable continuum model (CPCM) with water as the solvent.[39,40] UV−vis

DOI: 10.1021/acsearthspacechem.9b00235
ACS Earth Space Chem. 2019, 3, 2472−2481

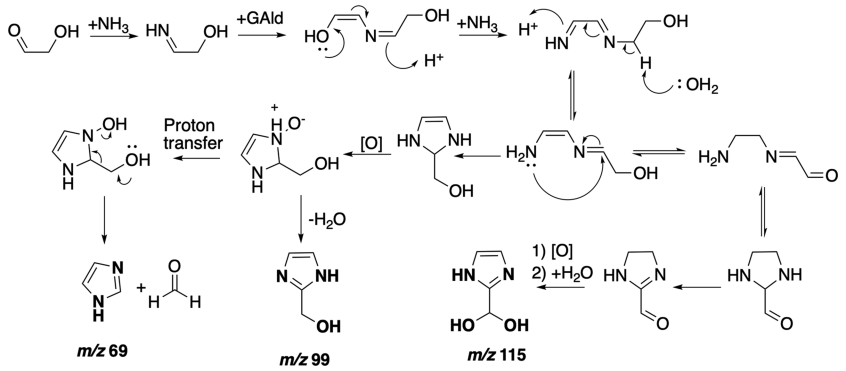

Figure 2. Proposed mechanism for the formation of imidazoles in the GAld + AS system. Structures in bold with m/z labels indicate compounds identified in this work.

absorption plots based on these calculations were generated according to the protocol implemented in GaussView.[41] To construct simulated absorption spectra, a Gaussian broadening function was applied to each excitation[38]

$$\varepsilon_i(\tilde{\nu}) = \frac{\sqrt{\pi}\cdot e^2\cdot N}{1000\cdot \ln(10)\cdot c^2\cdot m_e}\frac{f_i}{\sigma}\exp\left[-\left(\frac{\tilde{\nu}-\tilde{\nu}_i}{\sigma}\right)^2\right]$$

where ε is the extinction coefficient, e is the fundamental unit of charge, c is the speed of light, N is Avogadro's number, m_e is the electron mass, and f_i and $\tilde{\nu}_i$ are the oscillator strength and excitation energy (in wavenumbers), respectively, corresponding to the electronic excitation of interest. The width of the gaussian curve is denoted by σ, which is the standard deviation in wavenumbers. In this work, we used the default value in GaussView 6 of σ = 0.4 eV. The overall spectrum ($\varepsilon(\tilde{\nu})$) was determined by summing the contributions of each excitation according to the following equation.

$$\varepsilon(\tilde{\nu}) = \sum_{i=1}^{n}\varepsilon_i(\tilde{\nu})$$

Natural transition orbital (NTO) analysis was performed for the compounds identified in this work.[42] Electron orbitals, including NTOs and molecular orbitals (MOs), were visualized using GaussView.[41] An isosurface value of 0.02 was used in visualizations.

The calculated absorption energies were somewhat overestimated compared to the experimental standards measured in this work. Previously, it has been shown that the ωB97X-D functional can overestimate excitation energies by ~0.36 eV root mean square error, with overestimations reported up to 0.8 eV.[43] In addition, the highly absorbing $\pi-\pi^*$ transition in pyrazine is typically overestimated by DFT methods.[44,45] In order to compare calculated spectra directly to experimental results, a -0.6 eV shift was applied to calculated excitation energies (see Figure S6). For reference, we have provided the nonshifted excitation energies and corresponding oscillator strengths in the Supporting Information.

3. RESULTS AND DISCUSSION

Upon drying, the Gly and GAld reaction mixtures formed a brown solid that resulted in a light brown aqueous solution when reconstituted in Milli-Q water. The HA reaction samples formed a white solid that was colorless when reconstituted. The product masses for the reactions of GAld or Gly with AS observed in this study are consistent with published masses, while the authors are not aware of any published HA + AS masses.[9,11,18,25,32] New structures proposed in this study can be found in Table S1, and extracted ion chromatograms (EICs) for each mass can be found in Figures S1–S3.

3.1. Gly + AS. The major products in the Gly + AS system are consistent with those that have been identified in the previous literature.[9,18] We propose two new imidazole derivatives at low intensity (m/z 99 and 129) in this system. For these compounds, ^{15}N experiments confirm the presence of two nitrogen atoms in each structure, thus supporting the imidazole backbone. In addition, fragmentation patterns of m/z 69 and 42 further confirm the parent ion breakdown into the imidazole present in the structure, and fragments of m/z 83 correspond to methylimidazole.[33] The formation of these compounds is likely to follow a similar mechanism to the imidazole derivatives observed in previous studies.[9,18]

While imidazole-based compounds have been established as major products present in the Gly + AS reaction system, we also observe a low-intensity signal that corresponds to pyrazine (m/z 81). This is confirmed by comparison to a standard prepared using 98% pyrazine reagent (Alfa Aesar). The pyrazine standard and observed m/z 81 both fragment to m/z 54 and elute at approximately 18 min (see Figure S1). This finding is supported by the observation by Hawkins et al. of methylpyrazines in the MGly + AS system under acidic conditions.[30] The formation mechanism in the Gly + AS system is likely to follow the same formation mechanism as that suggested for 2,5-dimethylpyrazine since the carbonyls are the relevant reaction sites, and the methyl groups do not participate in the reaction itself.[30] As stated previously, Hawkins et al. observed that high water content may suppress pyrazine formation in atmospheric systems; this detail may explain why previous studies on aqueous, bulk phase Gly + AS did not detect pyrazine formation.[30]

3.2. GAld + AS. Aliphatic heterocycles have been previously observed in atmospheric aerosol mimics of the GAld + AS system,[25] but aromatic heterocycles have yet to be identified. Aromatic molecule formation is thought to be inaccessible due to the lack of a second carbonyl on the GAld molecule,[25] but we provide evidence to support the formation of both imidazole and pyrazine derivatives in the GAld + AS system. Similar to the Gly + AS system, imidazole derivatives (m/z 69, 99, and 115) are observed. A mass at m/z 69 was observed by Yi et al., but the authors did not propose a structure for this mass.[25] However, through the use of MS/MS, ^{15}N experiments, and comparison to a standard prepared using 99% imidazole (Sigma-Aldrich), we have identified this mass as

DOI: 10.1021/acsearthspacechem.9b00235
ACS Earth Space Chem. 2019, 3, 2472−2481

imidazole. Figure 2 shows a possible mechanism for the formation of imidazole and imidazole derivatives (m/z 99 and 115) in the GAld + AS system. The presence of 2-hydroxymethylimidazole was also confirmed by comparison with a standard (Sigma-Aldrich).

To produce m/z 99, GAld first undergoes imine formation. The imine then condenses with an additional GAld molecule, where subsequent dehydration produces the conjugated enol intermediate. An ensuing series of proton transfers, cyclization, and subsequent oxidation results in the stable aromatic 2-hydroxymethylimidazole product (m/z 99). Alternatively, the conjugated enol intermediate can tautomerize to form an aldehyde and the imidazole ring in hydrated imidazole-2-carboxaldehyde (m/z 115). As with the Gly + AS system, it is also possible for an alternate oxidation pathway to occur that cleaves formaldehyde from the compound to produce imidazole (m/z 69); the formaldehyde is likely lost to evaporation during the sample drying process and is too small for the MS to detect even if it remains in the sample.[9]

In addition to the imidazole derivatives found in the GAld + AS system, pyrazine derivatives are also observed. An MS/MS signal of m/z 81 fragments to m/z 54 and elutes at approximately 18 min (see Figure S2), which matches the fragmentation and retention time of the pyrazine standard. Furthermore, ^{15}N experiments reveal that two nitrogen atoms are present in this compound, thus further supporting the presence of pyrazine. Based on their fragmentation patterns (see Figure 3), the structures for m/z 125, 143, and 185 can be identified as pyrazine derivatives. Though Yi et al. proposed oxazine-based structures for m/z 143 and 185,[25] these fragmentation data support the observation of pyrazine derivatives. Each of these compounds fragments to m/z 80 during MS/MS analysis, which is typical of a pyrazine derivative. If these compounds contained oxazine within their structures, then it is highly unlikely that they would all fragment to m/z 80 based on their chemical structures. While m/z 143 was not identified in this study, the similarity of its fragmentation pattern to pyrazine (m/z 81) and pyrazine derivatives (m/z 125 and 185) suggests that it contains a pyrazine ring rather than an oxazine ring.

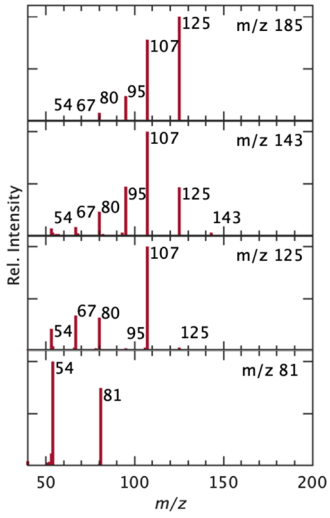

Figure 3. MS/MS data for pyrazine-containing compounds within the GAld + AS system. The similarities in the fragment masses indicate common structural features. All labeled peaks have an intensity above zero but may not be visible on the scale shown.

Though the formation of pyrazine and its derivatives has not been previously identified in aerosol mimics, Yu et al. reported that reactions between glycolaldehyde and hydroxyacetone in the presence of ammonia can produce methylated pyrazine in food chemistry.[46] While the mechanism they propose is not likely to occur in this slightly acidic system, the mechanism in Figure 4 shows a pathway for pyrazine and pyrazine derivatives to form under these reaction conditions. Amine-substituted glycolaldehyde (aminoacetaldehyde) undergoes dimerization followed by double dehydration. From this step, the intermediate can either oxidize to form pyrazine (m/z 81) or nucleophilically attack a GAld molecule via a tautomer. After subsequent dehydration and aromatization, m/z 125 is formed, with which another GAld unit can then react to form m/z 185.

3.3. HA + AS. The HA reaction system has not been studied in as much detail as the other small water-soluble aldehydes,[7,32,47] but it is reasonable to expect that its products have many similar functional groups to the other carbonyl systems discussed herein. HA is not a dicarbonyl and contains a ketone functional group rather than an aldehyde, so it does not react as quickly with ammonium in the dilute aqueous phase as Gly and MGly. However, reactions proceed orders of magnitude more quickly during the drying process than in the dilute solution, so many products are observed that are otherwise only seen after several months of dark reaction in the aqueous phase.[7,48] The products identified in this reaction system are shown in Figure 5, along with their formation pathways.

One of the masses observed via SFC-MS includes m/z 75, which corresponds to the HA monomer and indicates that not all of the original carbonyl reacted with ammonium during drying. HA can dimerize and then dehydrate to form an open-chain oligomer (m/z 131), which can further react with additional HA units (m/z 205) or ammonia to produce an imine (m/z 204). Like the initial amination of the GAld + AS system, HA can react with ammonia to produce aminoacetone (m/z 74). Notably, when aminoacetone dimerizes, it can form a heterocycle that is oxidized to 2,5-dimethylpyrazine (m/z 109), as shown to occur in the MGly system by Hawkins et al.[30] From m/z 131, furan derivatives (m/z 169) can be produced through aldol condensation pathways with HA or aminoacetone. Further reactions at the aldehyde carbonyl with additional HA units can produce extended furan derivatives (m/z 243).

Figure 5 also demonstrates a formation pathway for 1-(5-methyl-1*H*-imidazol-2-yl)ethanol (m/z 127), in which an aminoacetone dimer undergoes dehydration followed by tautomerization to form an imine, which acts as an electrophile for the amine nitrogen. The resulting heterocycle is then oxidized to 1-(5-methyl-1*H*-imidazol-2-yl)ethanol. Alternatively, this imidazole derivative could be formed via the reaction of 2-hydroxypropanal (in equilibrium with HA through an enol intermediate) and 1-propene-1,2-diamine (through imine formation and subsequent tautomerization) to form a cyclic intermediate that is then oxidized to the stable imidazole (m/z 127). Like the GAld + AS system, imidazole derivatives in the HA + AS system have not been reported previously, yet ample evidence is provided by SFC-MS/MS data and ^{15}N experiments to confirm the formation of methylated imidazole derivatives. The formation of this imidazole derivative (m/z 127), along with other observed

DOI: 10.1021/acsearthspacechem.9b00235
ACS Earth Space Chem. 2019, 3, 2472−2481

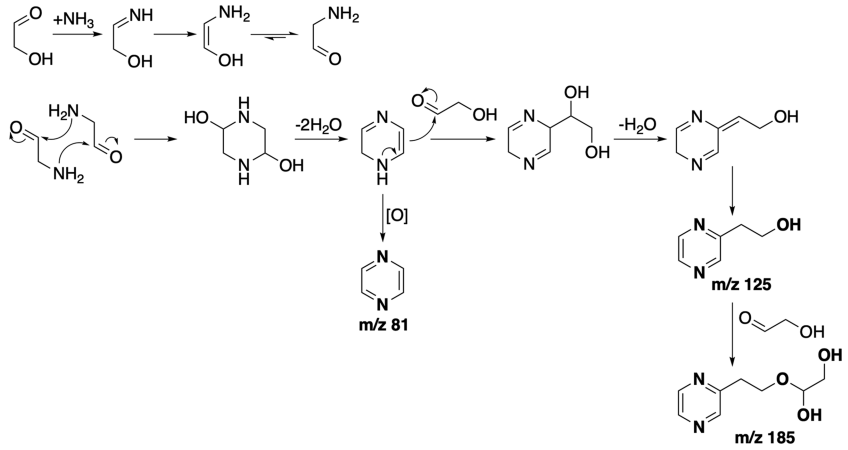

Figure 4. Proposed mechanism for the formation of pyrazine and its derivatives in the GAld + AS system. Structures in bold with m/z labels indicate compounds identified in this work.

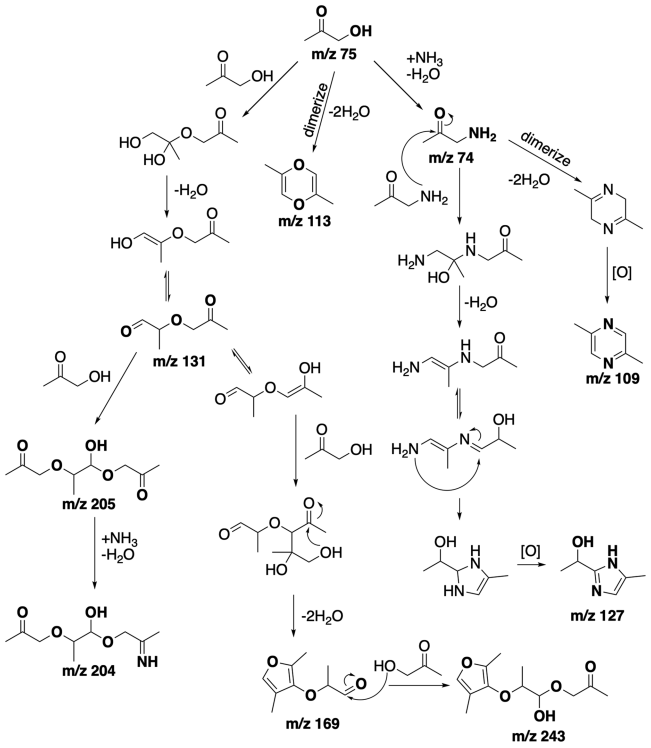

Figure 5. Proposed mechanism for HA + AS formation of open chains and heterocycles. Structures in bold with m/z labels indicate compounds identified in this work.

imidazoles (m/z 83, 97, and 113), is supported by MS/MS data. Fragmentation of the masses shows a common pattern (Figure S4), which includes fragment ions that indicate the presence of imidazole and methylated imidazole (m/z 42, 56, 69, and 83),[33] and ^{15}N experiments confirm the presence of two nitrogen atoms within their structures. Although HA + AS has been speculated to not contribute to major BrC chromophores like imidazole derivatives, it is important to note that there are multiple mechanistic pathways for imidazole formation in this system, even though the proposed mechanisms for HA + AS include steps that are less favorable than the corresponding α-dicarbonyl + AS imidazole formation pathways.

3.4. Light Absorption Calculations. The imidazole and pyrazine reaction products identified herein are further supported by the fact that the Gly + AS, GAld + AS, and HA + AS reaction systems absorb light in the BrC region (see Figure S5). The absorption spectra of the compounds identified in Table S1 were calculated using time-dependent density functional theory (see Figures S7−S9). The calculated absorption spectra indicate that pyrazine, furan, and imidazole derivatives exhibit high absorptivity in the region from 200 to 300 nm. When these aromatic heterocycles are alkyl-substituted, the absorption spectrum becomes red-shifted into the actinic region as shown in Figure 6. This indicates that these compounds likely contribute to BrC absorption in the Gly + AS, GAld + AS, and HA + AS mixtures studied in this work.

Pyrazine absorbs light in the actinic region, with a peak centered at 255 nm corresponding to the $\pi-\pi^*$ transition. The $n-\pi^*$ excitation centered at 341 nm has a small oscillator strength, which may contribute to the absorption tail into the visible spectrum. This peak energy, however, is slightly underestimated and is likely to appear at somewhat shorter wavelengths in aqueous solutions. The excitation is typically observed at 312 nm in aqueous solutions, where hydrogen bonds between solvent water and nitrogen lone pairs blue-shift the excitation.[44,49,50] Further discussion on pyrazine excitation wavelengths is included in the Supporting Information. The substituted pyrazines identified in Table S1 absorb even further into the actinic region, with the $\pi-\pi^*$ transition maxima shifting from 255 to 264 nm. To visualize the change in electron density upon absorption, a natural transition orbital analysis was performed. The highest occupied and lowest unoccupied transition orbitals (HOTO and LUTO, respectively) correspond to a one-electron representation of the change in electron density from the ground to excited state (i.e., a single particle-hole excitation) and are provided for representative compounds in Figure 7. As shown in the pyrazine transition orbitals, the electron density is more delocalized upon alkyl substitution. The red-shift in absorption energy occurs due to coupling between the π-orbital localized on the pyrazine ring and the highest occupied molecular orbital (HOMO) of the substituent group, which includes the p_z orbitals of the proximal carbon and oxygen atoms. This coupling between occupied states raises the energy of the occupied π-orbital that contributes the most to the excitation

DOI: 10.1021/acsearthspacechem.9b00235
ACS Earth Space Chem. 2019, 3, 2472−2481

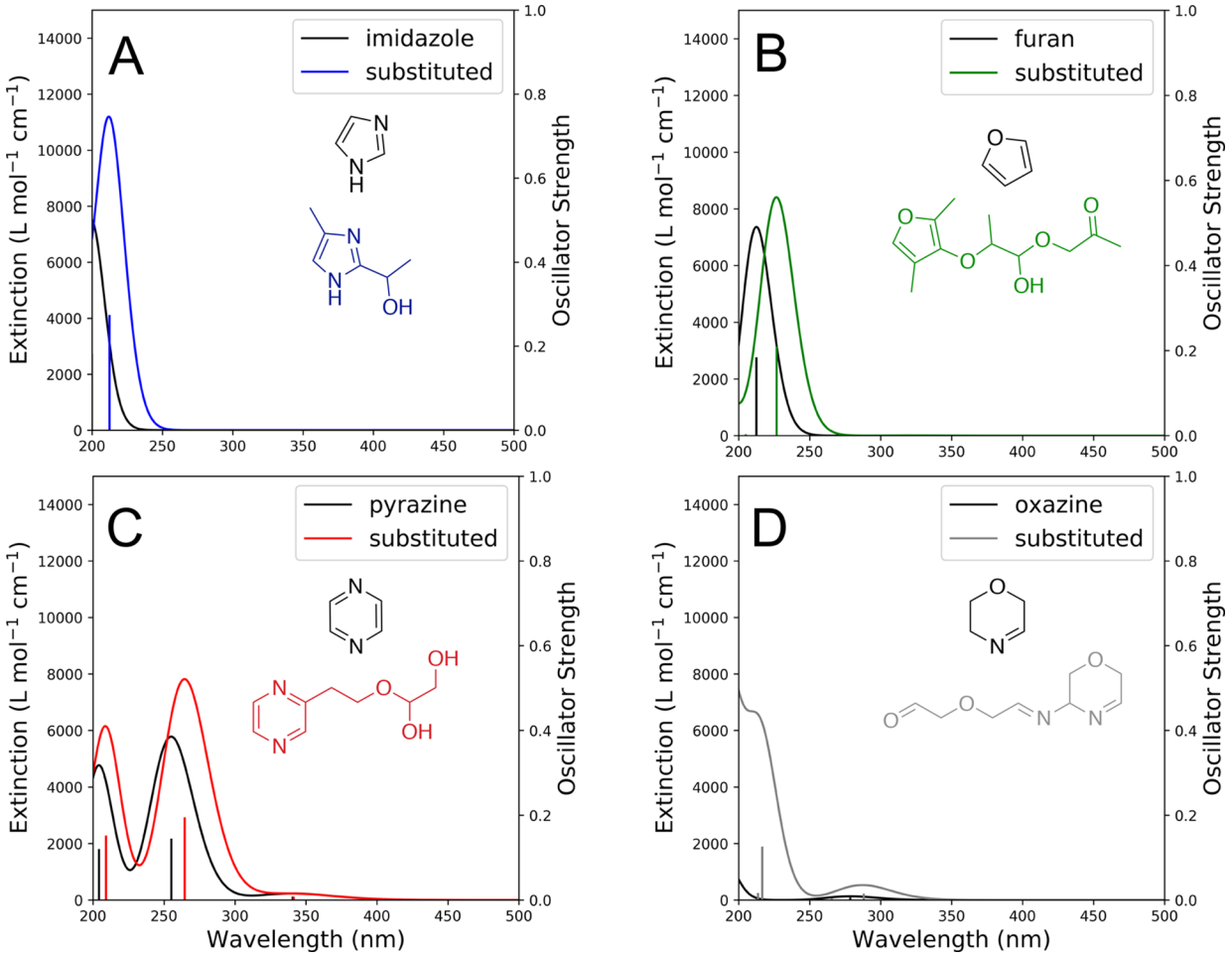

Figure 6. Calculated absorption spectra for aromatic heterocycles with and without substituent groups for (A) imidazole, derivative in blue, (B) furan, derivative in green, (C) pyrazine, derivative in red, and (D) oxazine, derivative in gray. The calculated vertical excitation energies are shown as sticks, with oscillator strengths corresponding to the right *y* axis.

(as shown in Figure S12). The virtual π^* orbital involved in the excitation is less coupled to the substituent group, so the energy of the orbital remains unchanged. Because the energy gap between these orbitals is smaller upon substitution, the excitation in the pyrazine derivative is red-shifted compared to that in pyrazine. The red-shift in absorption spectra indicates that pyrazine and its derivatives identified in this work are responsible for light absorption in the Gly + AS, GAld + AS, and HA + AS mixtures.

Furan derivatives were identified in the HA + AS system, and as shown in Figure 6, these aromatic heterocycles are also likely to contribute to light absorption into the BrC region. While furan absorbs light at 212 nm, substitution red-shifts the excitation to 226 nm. Upon substitution, the occupied and virtual π-orbitals in the furan ring can couple to the *p* orbitals of neighboring carbon and oxygen atoms of the substituent group (shown in Figure 7). As a result of the decreased orbital energy gap, the substituted furans absorb longer wavelength light, and their absorption spectra shifts toward the visible region.

As shown in Figure 6, the calculated spectrum for imidazole does not exhibit significant absorption in the BrC region. Instead, the maximum absorption peak is situated at 200 nm, which is in agreement with experimental values.[51] However, the substituted imidazoles identified herein do absorb into the BrC region. For example, the imidazole derivative in Figure 6 exhibits a $\pi-\pi^*$ transition peak centered at 212 nm. Like the other aromatic heterocycles, the occupied and virtual π-orbitals in the imidazole couple to neighboring carbon and oxygen atoms upon substitution. As a result, the excitation energy becomes red-shifted. In addition, the calculated oscillator strength (absorption intensity) for the $\pi-\pi^*$ transition in imidazole derivatives is fairly large compared to the other compounds considered in this study. The imidazole compounds have very high absorptivity coefficients, so even small concentrations will absorb significantly in the atmosphere.[52] It is likely that further substitution and conjugation of the molecule will shift this absorbance to lower energies, and unidentified substituted imidazoles within this system may be present. An example of such a compound is provided in Figure S14. Thus, it is expected that imidazole derivatives identified in this work are responsible for light absorption around 212 nm in Gly + AS, GAld + AS, and HA + AS mixtures, and further substituted imidazole compounds that may be present could contribute to light absorption at higher wavelengths.

Previously identified products in the GAld + AS system are open-chain acetal and amine oligomers and aliphatic heterocycles.[7,25,53] Light absorption spectra for several of these compounds were also calculated. In the case that π-conjugation extends across multiple bonds in an oligomer, it is possible for there to be significant absorptivity in the BrC region. However, in general, the open-chain acetal and amine oligomers did not

DOI: 10.1021/acsearthspacechem.9b00235
ACS Earth Space Chem. 2019, 3, 2472−2481

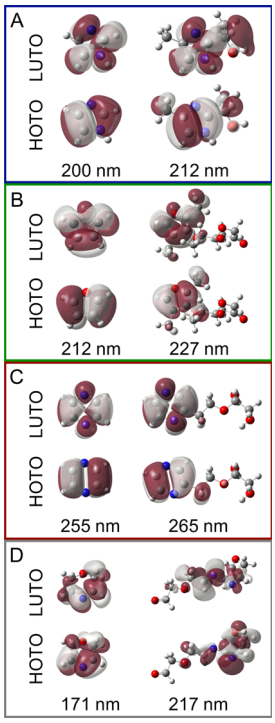

Figure 7. Natural transition orbitals (NTO) for the excitations with highest intensity shown in Figure 6 for the (A) imidazole + derivative, (B) furan + derivative, (C) pyrazine + derivative, and (D) oxazine + derivative. An isosurface value of 0.02 was used to generate the plots.

significantly absorb light in the ultraviolet or visible region (see Figures S10 and S11), indicating that the observed absorption likely arises from pyrazine, imidazole, and furan reaction products.

On the other hand, non-aromatic oxazine derivatives were also proposed by Yi et al. as potential BrC reaction products, and the absorption spectra for several of these compounds were calculated.[25] The absorption maximum for the $\pi-\pi^*$ transition is centered at 216 nm, as shown in Figure 6D. There is an $n-\pi^*$ excitation with a small oscillator strength near 290 nm that could enable these compounds to absorb into the visible region. The peak around 216 nm occurs at a similar range as the imidazole derivatives, albeit with a significantly smaller absorption intensity (i.e., approximately 60% smaller oscillator strength on average, as shown in Table S6). The smaller oscillator strength can be attributed to the smaller amount of spatial overlap between the HOTO and LUTO for the oxazine derivative compared to the other heterocycle derivatives. As shown in Figure 7, the HOTO is more localized on the oxazine moiety, while the LUTO is more localized on the imine moiety. The oxazine peak near 290 nm is somewhat near the peak maximum for the pyrazine derivatives (around 260 nm), and like imidazoles, the pyrazine derivatives exhibit a significant absorption intensity in this region. The oxazine derivatives exhibit an average oscillator strength that is only 7% that of pyrazines in this region. While the low molecular absorptivity of previously proposed oxazines in the actinic region does not definitively rule out the formation of oxazines in this system,[25] it does indicate that the imidazoles and pyrazines are overwhelmingly contributing to the observed light absorption.

The GAld + AS and HA + AS systems do not absorb light to the same extent as MGly and Gly, which indicates that many of the products of this reaction are not chromophoric or are chromophores that are found in very small concentrations, as was observed via MS/MS. However, there are chromophoric products within this system that absorb light further into the actinic region; this absorbance is not explained by the oxazine and open-chain oligomers previously observed.[25,53] Previous studies disagree when it comes to the significance of the HA + AS system as a source of atmospheric BrC as compared to the other carbonyl + AS systems based on its light absorption properties. For example, Gao et al. found that this system did not absorb significant light, while Powelson et al. reported that its potential for BrC production may be on par with GAld + AS.[7,32] The HA + AS mixture does absorb light in the mid-UV region and exhibits some BrC character (see Figure S5). The structures identified in this study support the conclusion that while the light absorbance may be lower than that of the Gly + AS system, the HA + AS system is likely to contribute to BrC absorption in the atmosphere. These newly identified aromatic imidazole and pyrazine derivatives absorb light in the actinic region and can help to fill the gap between previous knowledge and experiments.

4. CONCLUSIONS

It has previously been thought that small atmospheric aldehydes lacking an α-dicarbonyl (e.g., GAld and HA) cannot form aromatic heterocycles such as imidazoles in the presence of ammonium or amines.[25] This work shows that these reactions are possible. Aromatic heterocycles such as imidazole and pyrazine derivatives in sparsely studied carbonyl + AS systems has been identified in atmospheric aerosol mimics for the first time. Though lacking the reactivity that comes from the second carbonyl moiety in the extensively studied MGly and Gly systems, this product formation occurs in both the GAld and HA systems. In bulk phase reactions, these compounds are likely to form much more slowly than comparable compounds in the MGly or Gly + AS systems, but their formation can be accelerated by rapidly drying the aqueous solution, simulating cloud processing.

The addition of the formation mechanisms for these small heterocyclic compounds into our scientific knowledge may help us to further understand the light absorbing properties of atmospheric droplets. As conjugated imine systems and N-containing aromatics have been thought to provide some of the major absorbing species in the MGly + AS and Gly + AS systems, the discovery of these compounds in the HA and GAld systems could play an important role in informing more detailed characteristics of BrC formation in global climate models, especially in regions susceptible to generating these carbonyl precursors.

The observation and identification of these cyclic compounds has significant impacts on our understanding of the formation and abundance of these BrC compounds. Since α-hydroxycarbonyl compounds can form 5- and 6-membered heterocyclic rings in the presence of ammonia, it is likely that analogous compounds can also be formed in the presence of other simple amines such as methylamine and amino acids. As these amines are also abundantly found in the atmosphere,[7] these reactions highlight an additional area of study for potential BrC formation in order to expand our knowledge on their significance in global climate modeling.

DOI: 10.1021/acsearthspacechem.9b00235
ACS Earth Space Chem. 2019, 3, 2472−2481

■ ASSOCIATED CONTENT

Supporting Information

The Supporting Information is available free of charge on the ACS Publications website at DOI: 10.1021/acsearthspacechem.9b00235.

Extracted ion chromatograms, structures, and fragmentation information for identified products; absorbance spectra for reaction mixtures; comparisons between calculated and experimental UV−vis absorption spectra; calculated UV−vis absorption data for all identified products and other compounds mentioned in this work; and orbital pictures describing the effect of substitution on pyrazine electronic states involved in absorption (PDF)

■ AUTHOR INFORMATION

Corresponding Author

*E-mail: gallowam@lafayette.edu. Phone: (610)330-5206. Fax: (610)330-5714.

ORCID

Daniel R. Griffith: 0000-0002-0361-8290

Melissa M. Galloway: 0000-0002-8518-1888

Present Address

†Present address: Department of Chemistry, University of Pennsylvania, Philadelphia, Pennsylvania 19104, United States.

Author Contributions

‡D.N.G. and J.R.S. contributed equally to this work.

Author Contributions

The manuscript was written through contributions of all authors. All authors have given approval to the final version of the manuscript.

Notes

The authors declare no competing financial interest.

■ ACKNOWLEDGMENTS

Funding for this work was provided by the National Science Foundation (MRI-1626100). The authors would like to thank Dr. Charles Nutaitis for contributions to proposed mechanistic pathways and Dr. Joseph Woo for helpful discussions about this work.

■ REFERENCES

(1) Hallquist, M.; Wenger, J. C.; Baltensperger, U.; Rudich, Y.; Simpson, D.; Claeys, M.; Dommen, J.; Donahue, N. M.; George, C.; Goldstein, A. H.; Hamilton, J. F.; Herrmann, H.; Hoffmann, T.; Iinuma, Y.; Jang, M.; Jenkin, M. E.; Jimenez, J. L.; Kiendler-Scharr, A.; Maenhaut, W.; McFiggans, G.; Mentel, T. F.; Monod, A.; Prévôt, A. S. H.; Seinfeld, J. H.; Surratt, J. D.; Szmigielski, R.; Wildt, J. The formation, properties and impact of secondary organic aerosol: current and emerging issues. *Atmos. Chem. Phys.* **2009**, *9*, 5155−5236.

(2) Jimenez, J. L.; Canagaratna, M. R.; Donahue, N. M.; Prevot, A. S. H.; Zhang, Q.; Kroll, J. H.; DeCarlo, P. F.; Allan, J. D.; Coe, H.; Ng, N. L.; Aiken, A. C.; Docherty, K. S.; Ulbrich, I. M.; Grieshop, A. P.; Robinson, A. L.; Duplissy, J.; Smith, J. D.; Wilson, K. R.; Lanz, V. A.; Hueglin, C.; Sun, Y. L.; Tian, J.; Laaksonen, A.; Raatikainen, T.; Rautiainen, J.; Vaattovaara, P.; Ehn, M.; Kulmala, M.; Tomlinson, J. M.; Collins, D. R.; Cubison, M. J.; Dunlea, J. E.; Huffman, J. A.; Onasch, T. B.; Alfarra, M. R.; Williams, P. I.; Bower, K.; Kondo, Y.; Schneider, J.; Drewnick, F.; Borrmann, S.; Weimer, S.; Demerjian, K.; Salcedo, D.; Cottrell, L.; Griffin, R.; Takami, A.; Miyoshi, T.; Hatakeyama, S.; Shimono, A.; Sun, J. Y.; Zhang, Y. M.; Dzepina, K.; Kimmel, J. R.; Sueper, D.; Jayne, J. T.; Herndon, S. C.; Trimborn, A. M.; Williams, L. R.; Wood, E. C.; Middlebrook, A. M.; Kolb, C. E.; Baltensperger, U.; Worsnop, D. R. Evolution of Organic Aerosols in the Atmosphere. *Science* **2009**, *326*, 1525−1529.

(3) Ervens, B.; Turpin, B. J.; Weber, R. J. Secondary organic aerosol formation in cloud droplets and aqueous particles (aqSOA): a review of laboratory, field and model studies. *Atmos. Chem. Phys.* **2011**, *11*, 11069−11102.

(4) Laskin, A.; Laskin, J.; Nizkorodov, S. A. Chemistry of atmospheric brown carbon. *Chem. Rev.* **2015**, *115*, 4335−4382.

(5) Andreae, M. O.; Gelencsér, A. Black carbon or brown carbon? The nature of light-absorbing carbonaceous aerosols. *Atmos. Chem. Phys.* **2006**, *6*, 3131−3148.

(6) Lee, A. K. Y.; Zhao, R.; Li, R.; Liggio, J.; Li, S.-M.; Abbatt, J. P. D. Formation of Light Absorbing Organo-Nitrogen Species from Evaporation of Droplets Containing Glyoxal and Ammonium Sulfate. *Environ. Sci. Technol.* **2013**, *47*, 12819−12826.

(7) Powelson, M. H.; Espelien, B. M.; Hawkins, L. N.; Galloway, M. M.; De Haan, D. O. Brown carbon formation by aqueous-phase carbonyl compound reactions with amines and ammonium sulfate. *Environ. Sci. Technol.* **2014**, *48*, 985−993.

(8) Galloway, M. M.; Huisman, A. J.; Yee, L. D.; Chan, A. W. H.; Loza, C. L.; Seinfeld, J. H.; Keutsch, F. N. Yields of oxidized volatile organic compounds during the OH radical initiated oxidation of isoprene, methyl vinyl ketone, and methacrolein under high-NO_x conditions. *Atmos. Chem. Phys.* **2011**, *11*, 10779−10790.

(9) Yu, G.; Bayer, A. R.; Galloway, M. M.; Korshavn, K. J.; Fry, C. G.; Keutsch, F. N. Glyoxal in aqueous ammonium sulfate solutions: Products, kinetics and hydration effects. *Environ. Sci. Technol.* **2011**, *45*, 6336−6342.

(10) Ortiz-Montalvo, D. L.; Lim, Y. B.; Perri, M. J.; Seitzinger, S. P.; Turpin, B. J. Volatility and Yield of Glycolaldehyde SOA Formed through Aqueous Photochemistry and Droplet Evaporation. *Aerosol Sci. Technol.* **2012**, *46*, 1002−1014.

(11) Kampf, C. J.; Filippi, A.; Zuth, C.; Hoffmann, T.; Opatz, T. Secondary brown carbon formation via the dicarbonyl imine pathway: nitrogen heterocycle formation and synergistic effects. *Phys. Chem. Chem. Phys.* **2016**, *18*, 18353−18364.

(12) De Haan, D. O.; Corrigan, A. L.; Tolbert, M. A.; Jimenez, J. L.; Wood, S. E.; Turley, J. J. Secondary Organic Aerosol Formation by Self-Reactions of Methylglyoxal and Glyoxal in Evaporating Droplets. *Environ. Sci. Technol.* **2009**, *43*, 8184−8190.

(13) De Haan, D. O.; Corrigan, A. L.; Smith, K. W.; Stroik, D. R.; Turley, J. J.; Lee, F. E.; Tolbert, M. A.; Jimenez, J. L.; Cordova, K. E.; Ferrell, G. R. Secondary Organic Aerosol-Forming Reactions of Glyoxal with Amino Acids. *Environ. Sci. Technol.* **2009**, *43*, 2818−2824.

(14) Galloway, M. M.; Chhabra, P. S.; Chan, A. W. H.; Surratt, J. D.; Flagan, R. C.; Seinfeld, J. H.; Keutsch, F. N. Glyoxal uptake on ammonium sulphate seed aerosol: reaction products and reversibility of uptake under dark and irradiated conditions. *Atmos. Chem. Phys.* **2009**, *9*, 3331−3345.

(15) Nozière, B.; Dziedzic, P.; Córdova, A. Products and Kinetics of the Liquid-Phase Reaction of Glyoxal Catalyzed by Ammonium Ions (NH_4^+). *J. Phys. Chem. A* **2009**, *113*, 231−237.

(16) Shapiro, E. L.; Szprengiel, J.; Sareen, N.; Jen, C. N.; Giordano, M. R.; McNeill, V. F. Light-absorbing secondary organic material formed by glyoxal in aqueous aerosol mimics. *Atmos. Chem. Phys.* **2009**, *9*, 2289−2300.

(17) De Haan, D. O.; Hawkins, L. N.; Kononenko, J. A.; Turley, J. J.; Corrigan, A. L.; Tolbert, M. A.; Jimenez, J. L. Formation of Nitrogen-Containing Oligomers by Methylglyoxal and Amines in Simulated Evaporating Cloud Droplets. *Environ. Sci. Technol.* **2011**, *45*, 984−991.

(18) Kampf, C. J.; Jakob, R.; Hoffmann, T. Identification and characterization of aging products in the glyoxal/ammonium sulfate system - implications for light-absorbing material in atmospheric aerosols. *Atmos. Chem. Phys.* **2012**, *12*, 6323−6333.

(19) Lin, P.; Laskin, J.; Nizkorodov, S. A.; Laskin, A. Revealing Brown Carbon Chromophores Produced in Reactions of Methyl-

DOI: 10.1021/acsearthspacechem.9b00235
ACS Earth Space Chem. 2019, 3, 2472−2481

glyoxal with Ammonium Sulfate. *Environ. Sci. Technol.* **2015**, *49*, 14257−14266.
(20) Maxut, A.; Nozière, B.; Fenet, B.; Mechakra, H. Formation mechanisms and yields of small imidazoles from reactions of glyoxal with NH_4^+ in water at neutral pH. *Phys. Chem. Chem. Phys.* **2015**, *17*, 20416−20424.
(21) Hawkins, L. N.; Lemire, A. N.; Galloway, M. M.; Corrigan, A. L.; Turley, J. J.; Espelien, B. M.; De Haan, D. O. Maillard Chemistry in Clouds and Aqueous Aerosol As a Source of Atmospheric Humic-Like Substances. *Environ. Sci. Technol.* **2016**, *50*, 7443−7452.
(22) Aiona, P. K.; Lee, H. J.; Leslie, R.; Lin, P.; Laskin, A.; Laskin, J.; Nizkorodov, S. A. Photochemistry of Products of the Aqueous Reaction of Methylglyoxal with Ammonium Sulfate. *ACS Earth Space Chem.* **2017**, *1*, 522−532.
(23) De Haan, D. O.; Hawkins, L. N.; Welsh, H. G.; Pednekar, R.; Casar, J. R.; Pennington, E. A.; de Loera, A.; Jimenez, N. G.; Symons, M. A.; Zauscher, M.; Pajunoja, A.; Caponi, L.; Cazaunau, M.; Formenti, P.; Gratien, A.; Pangui, E.; Doussin, J.-F. Brown Carbon Production in Ammonium- or Amine-Containing Aerosol Particles by Reactive Uptake of Methylglyoxal and Photolytic Cloud Cycling. *Environ. Sci. Technol.* **2017**, *51*, 7458−7466.
(24) De Haan, D. O.; Tapavicza, E.; Riva, M.; Cui, T.; Surratt, J. D.; Smith, A. C.; Jordan, M.-C.; Nilakantan, S.; Almodovar, M.; Stewart, T. N.; de Loera, A.; De Haan, A. C.; Cazaunau, M.; Gratien, A.; Pangui, E.; Doussin, J.-F. Nitrogen-Containing, Light-Absorbing Oligomers Produced in Aerosol Particles Exposed to Methylglyoxal, Photolysis, and Cloud Cycling. *Environ. Sci. Technol.* **2018**, *52*, 4061−4071.
(25) Yi, Y.; Cao, Z.; Zhou, X.; Xue, L.; Wang, W. Formation of aqueous-phase secondary organic aerosols from glycolaldehyde and ammonium sulfate/amines: A kinetic and mechanistic study. *Atmos. Environ.* **2018**, *181*, 117−125.
(26) Sareen, N.; Schwier, A. N.; Shapiro, E. L.; Mitroo, D.; McNeill, V. F. Secondary organic material formed by methylglyoxal in aqueous aerosol mimics. *Atmos. Chem. Phys.* **2010**, *10*, 997−1016.
(27) Trainic, M.; Abo Riziq, A.; Lavi, A.; Flores, J. M.; Rudich, Y. The optical, physical and chemical properties of the products of glyoxal uptake on ammonium sulfate seed aerosols. *Atmos. Chem. Phys.* **2011**, *11*, 9697−9707.
(28) Woo, J. L.; Kim, D. D.; Schwier, A. N.; Li, R.; McNeill, V. F. Aqueous aerosol SOA formation: impact on aerosol physical properties. *Faraday Discuss.* **2013**, *165*, 357−367.
(29) Rodriguez, A. A.; de Loera, A.; Powelson, M. H.; Galloway, M. M.; De Haan, D. O. Formaldehyde and Acetaldehyde Increase Aqueous-Phase Production of Imidazoles in Methylglyoxal/Amine Mixtures: Quantifying a Secondary Organic Aerosol Formation Mechanism. *Environ. Sci. Technol. Lett.* **2017**, *4*, 234−239.
(30) Hawkins, L. N.; Welsh, H. G.; Alexander, M. V. Evidence for pyrazine-based chromophores in cloud water mimics containing methylglyoxal and ammonium sulfate. *Atmos. Chem. Phys.* **2018**, *18*, 12413−12431.
(31) Woo, J. L.; McNeill, V. F. simpleGAMMA v1.0 − a reduced model of secondary organic aerosol formation in the aqueous aerosol phase (aaSOA). *Geosci. Model Dev.* **2015**, *8*, 1821−1829.
(32) Gao, Y.; Zhang, Y. Formation and photochemical investigation of brown carbon by hydroxyacetone reactions with glycine and ammonium sulfate. *RSC Adv.* **2018**, *8*, 20719−20725.
(33) Grace, D. N.; Sebold, M. B.; Galloway, M. M. Separation and detection of aqueous atmospheric aerosol mimics using supercritical fluid chromatography−mass spectrometry. *Atmos. Meas. Tech.* **2019**, *12*, 3841−3851.
(34) Grimme, S. Semiempirical GGA-type density functional constructed with a long-range dispersion correction. *J. Comput. Chem.* **2006**, *27*, 1787−1799.
(35) Chai, J.-D.; Head-Gordon, M. Long-range corrected hybrid density functionals with damped atom−atom dispersion corrections. *Phys. Chem. Chem. Phys.* **2008**, *10*, 6615−6620.
(36) Krishnan, R.; Binkley, J. S.; Seeger, R.; Pople, J. A. Self-consistent molecular orbital methods. XX. A basis set for correlated wave functions. *J. Chem. Phys.* **1980**, *72*, 650−654.
(37) McLean, A. D.; Chandler, G. S. Contracted Gaussian basis sets for molecular calculations. I. Second row atoms, Z=11−18. *J. Chem. Phys.* **1980**, *72*, 5639−5648.
(38) Frisch, M. J.; Trucks, G. W.; Schlegel, H. B.; Scuseria, G. E.; Robb, M. A.; Cheeseman, J. R.; Scalmani, G.; Barone, V.; Petersson, G. A.; Nakatsuji, H.; Li, X.; Caricato, M.; Marenich, A. V.; Bloino, J.; Janesko, B. G.; Gomperts, R.; Mennucci, B.; Hratchian, H. P.; Ortiz, J. V.; Izmaylov, A. F.; Sonnenberg, J. L.; Williams-Young, D.; Ding, F.; Lipparini, F.; Egidi, F.; Goings, J.; Peng, B.; Petrone, A.; Henderson, T.; Ranasinghe, D.; Zakrzewski, V. G.; Gao, J.; Rega, N.; Zheng, G.; Liang, W.; Hada, M.; Ehara, M.; Toyota, K.; Fukuda, R.; Hasegawa, J.; Ishida, M.; Nakajima, T.; Honda, Y.; Kitao, O.; Nakai, H.; Vreven, T.; Throssell, K.; Montgomery, J. A., Jr.; Peralta, J. E.; Ogliaro, F.; Bearpark, M. J.; Heyd, J. J.; Brothers, E. N.; Kudin, K. N.; Staroverov, V. N.; Keith, T. A.; Kobayashi, R.; Normand, J.; Raghavachari, K.; Rendell, A. P.; Burant, J. C.; Iyengar, S. S.; Tomasi, J.; Cossi, M.; Millam, J. M.; Klene, M.; Adamo, C.; Cammi, R.; Ochterski, J. W.; Martin, R. L.; Morokuma, K.; Farkas, O.; Foresman, J. B.; Fox, D. J. *Gaussian, 16*; Gaussian, Inc.: Wallingford, CT, 2016.
(39) Barone, V.; Cossi, M. Quantum Calculation of Molecular Energies and Energy Gradients in Solution by a Conductor Solvent Model. *J. Phys. Chem. A* **1998**, *102*, 1995−2001.
(40) Cossi, M.; Rega, N.; Scalmani, G.; Barone, V. Polarizable dielectric model of solvation with inclusion of charge penetration effects. *J. Chem. Phys.* **2001**, *114*, 5691−5701.
(41) Dennington, R.; Keith, T. A.; Millam, J. M. *Gaussview, 6.0.16*; Semichem Inc.: Shawnee Mission, KS, 2016.
(42) Martin, R. L. Natural transition orbitals. *J. Chem. Phys.* **2003**, *118*, 4775−4777.
(43) Jacquemin, D.; Moore, B., II; Planchat, A.; Adamo, C.; Autschbach, J. Performance of an Optimally Tuned Range-Separated Hybrid Functional for 0−0 Electronic Excitation Energies. *J. Chem. Theory Comput.* **2014**, *10*, 1677−1685.
(44) Weber, P.; Reimers, J. R. Ab Initio and Density Functional Calculations of the Energies of the Singlet and Triplet Valence Excited States of Pyrazine. *J. Phys. Chem. A* **1999**, *103*, 9821−9829.
(45) Ziegler, T.; Krykunov, M.; Cullen, J. The Application of Constricted Variational Density Functional Theory to Excitations Involving Electron Transitions from Occupied Lone-Pair Orbitals to Virtual π^* Orbitals. *J. Chem. Theory Comput.* **2011**, *7*, 2485−2491.
(46) Yu, A.-N.; Tan, Z.-W.; Wang, F.-S. Mechanistic studies on the formation of pyrazines by Maillard reaction between l-ascorbic acid and l-glutamic acid. *LWT–Food Sci. Technol.* **2013**, *50*, 64−71.
(47) Galloway, M. M.; Powelson, M. H.; Sedehi, N.; Wood, S. E.; Millage, K. D.; Kononenko, J. A.; Rynaski, A. D.; De Haan, D. O. Secondary Organic Aerosol Formation during Evaporation of Droplets Containing Atmospheric Aldehydes, Amines, and Ammonium Sulfate. *Environ. Sci. Technol.* **2014**, *48*, 14417−14425.
(48) Sedehi, N.; Takano, H.; Blasic, V. A.; Sullivan, K. A.; De Haan, D. O. Temperature- and pH-dependent aqueous-phase kinetics of the reactions of glyoxal and methylglyoxal with atmospheric amines and ammonium sulfate. *Atmos. Environ.* **2013**, *77*, 656−663.
(49) Zeng, J.; Hush, N. S.; Reimers, J. R Solvent Effects on Molecular and Ionic Spectra. VIII. The 1(n,π^*) Excited States of Pyridazine in Water. *J. Phys. Chem.* **1996**, *100*, 9561−9567.
(50) Liu, T.; Han, W.-G.; Himo, F.; Ullmann, G. M.; Bashford, D.; Toutchkine, A.; Hahn, K. M.; Noodleman, L. Density Functional Vertical Self-Consistent Reaction Field Theory for Solvatochromism Studies of Solvent-Sensitive Dyes. *J. Phys. Chem. A* **2004**, *108*, 3545−3555.
(51) Barbatti, M.; Lischka, H.; Salzmann, S.; Marian, C. M. UV excitation and radiationless deactivation of imidazole. *J. Chem. Phys.* **2009**, *130*, 034305.
(52) Ackendorf, J. M.; Ippolito, M. G.; Galloway, M. M. pH Dependence of the Imidazole-2-carboxaldehyde Hydration Equili-

DOI: 10.1021/acsearthspacechem.9b00235
ACS Earth Space Chem. 2019, 3, 2472−2481

brium: Implications for Atmospheric Light Absorbance. *Environ. Sci. Technol. Lett.* **2017**, *4*, 551−555.
(53) Kua, J.; Galloway, M. M.; Millage, K. D.; Avila, J. E.; De Haan, D. O. Glycolaldehyde Monomer and Oligomer Equilibria in Aqueous Solution: Comparing Computational Chemistry and NMR Data. *J. Phys. Chem. A* **2013**, *117*, 2997−3008.

DOI: 10.1021/acsearthspacechem.9b00235
ACS Earth Space Chem. 2019, 3, 2472−2481